Rev.Adv.Mater.Sci. 18(2008) 433-438

# THE INFLUENCE OF INCREASING COPPER ADDITION ON THE PROPERTIES OF (NiCu)ZrTiAlSi AMORPHOUS ALLOYS

**Tomasz Czeppe[1], Anna Sypień[1], Chinh Singh[2] and Patrick Ochin[3]**

[1]Institute of Metallurgy and Materials Science PAS, Reymonta 25 St, 30-059 Kraków, Poland
[2]Dept. of General Physics, Eötvös University, Pázmány P. Sétány 1/A, 1117 Budapest, Hungary
[3]Centre d'Etudes de Chimie Métallurgique, UPR 2801, 15, Rue G. Urbain, 94407 Vitry-sur-Seine, Cedex – France

*Received: March 29, 2008*

**Abstract.** Ni based BMG's with Cu addition may form a composite structure containing particles (dendrites) of a ductile phase in an amorphous matrix. Alloys of $(Ni_{1-x}Cu_x)_{60}(Zr_{18}Ti_{13})Al_5Si_4$ composition, with copper content increasing from 8 to 23 at.% were investigated in the form of ribbons produced by melt spinning and bulk samples solidified in a copper mould. Increasing Cu content resulted in gradually decreasing melting, glass transition and primary crystallization temperatures, while supercooled liquid range $\Delta T$ increased. The microhardness and Young modulus of the ribbons slightly decreased with the Cu content increase. The 0.65 value of the reduced glass transition temperature remained independent of the Cu addition. Bulk samples underwent partial crystallization of the dendrites. The lowest amorphous phase amount revealed the alloy with 25 at.% of the Cu addition.

## 1. INTRODUCTION

Similarly to glasses on the base of Fe and Ti, amorphous or partially nanocrystalline, NiZrTi- based alloys can reveal high strength and hardness, high thermal stability of the amorphous phase and especially good resistance in corrosive conditions [1]. Some additions like Hf, Y, Si or Sn increase glass forming ability [2-4], Si may lower mechanical properties of the alloys [5,6] but in many cases increases the achievable diameter of the BMG's [7]. The Cu additions may influence the crystallization process as well as the strength and corrosion resistance of the alloys [5,6]. The Al addition promotes lower temperature of crystallization [8].

The work was undertaken to investigate the influence of gradually increasing Cu content on the properties of alloys of nominal composition $(Ni_{1-x}Cu_x)_{60}(Zr_{18}Ti_{13})Al_5Si_4$ with the content of copper changing from 8 to 23 at.%. Alloys of similar Ni-based compositions were presented in the literature as potential amorphous composites [9].

## 2. EXPERIMENTAL

The alloys were prepared from components of 3N and 4N purity, by melting in an induction furnace, under argon atmosphere. The materials were several times re-melted by the levitation method and cast in the copper mould. The bulk samples were 2.5 mm in diameter. The ribbon samples were spun in He gas atmosphere on the CuCoBe disc rotating with the linear velocity of 19 m/s. The ribbons produced were 9 mm wide and 50 mm thick.

Phase analysis was performed with the Philips PW 1830 diffractometer, Co $K_\alpha$ radiation was used. The electron microscopes: transmission Philips CM20 (200 KV) equipped with the EDAX Phoenix

Corresponding author: Tomasz Czeppe, e-mail: nmczeppe@imim-pan.krakow.pl

**Table 1.** Results of the thermal analysis of the ribbons. Glass transition temperature ($T_g$), primary crystallization temperature ($T_x$), solidus and liquidus temperatures ($T_s$ and $T_l$), enthalpies of the first effect ($\Delta H_{cr.1}$), of the completed crystallization ($\Delta H^{tot.}_{cr.}$) and of the melting ($\Delta H_m$).

| Alloy | $T_g$ [°C] | $T_x$ [°C] | $\Delta H_{cr.1}$ [J/g] | $\Delta H^{tot.}_{cr.}$ [J/g] | Heating 20 deg/min | | Cooling 20 deg/min | | $\Delta H_m$ [J/g] |
|---|---|---|---|---|---|---|---|---|---|
| | | | | | $T_s$ [°C] | $T_l$ [°C] | $T_s$ [°C] | $T_l$ [°C] | |
| **2A-1** | 557.7 | 573.3 | 77.5 | 65.2 | 1000.6 | 1182.9 | 980.4 | 1082.3 | 48.2 |
| **2A-2** | 553.9 | 568.4 | 72.1 | 94.3 | 994.3 | 1170.6 | 974.1 | 1073.1 | 72.9 |
| **2A-3** | 533.2 | 558.6 | 82.4 | 115.3 | 984.3 | 1160.2 | 970.4 | 1066.0 | 60.5 |
| **2A-4** | 530.5 | 552.8 | 84.1 | 139.3 | 972.7 | 1151.6 | 962.7 | 1057.4 | 75.6 |

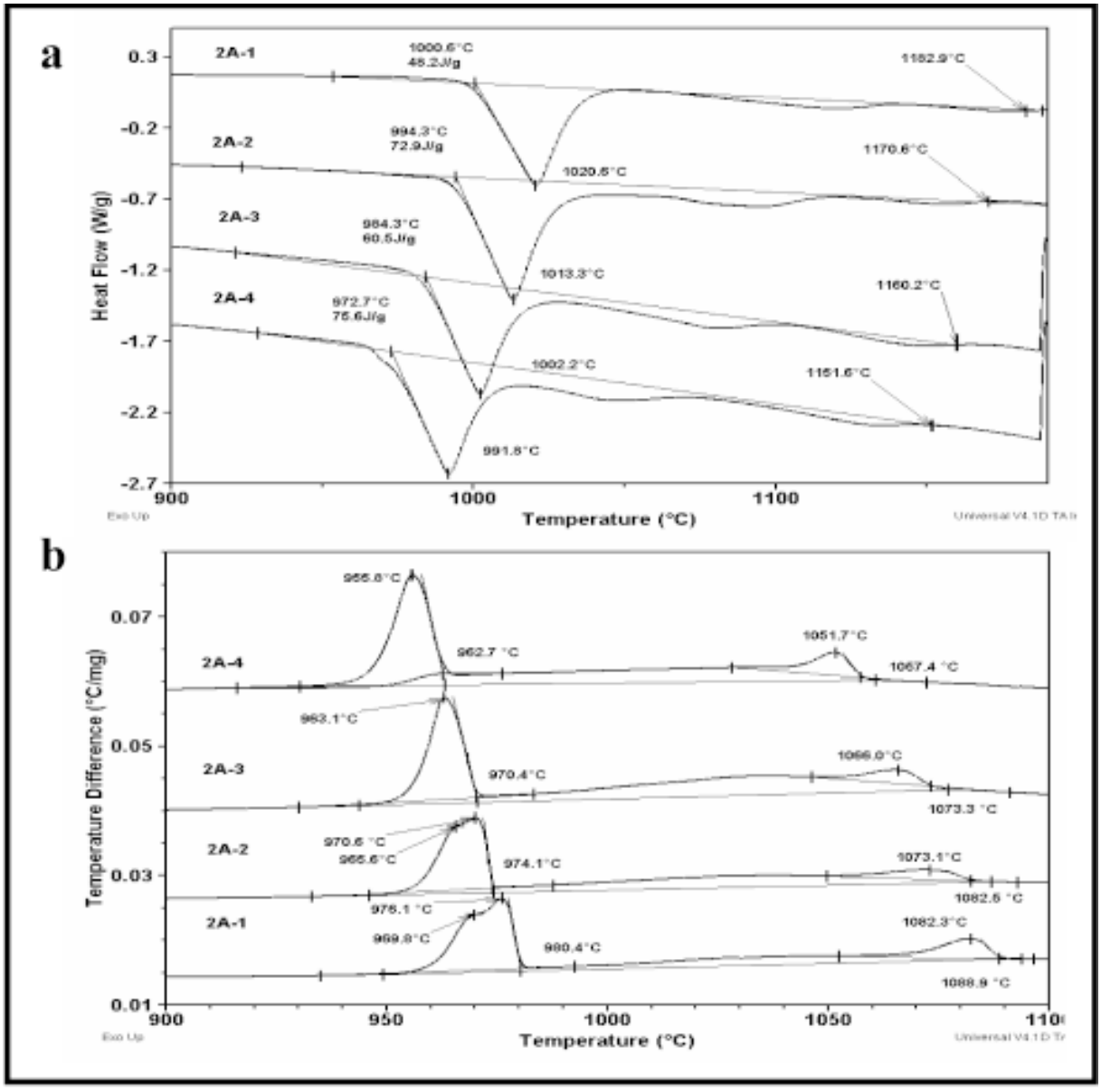


**Fig. 1.** Thermal analysis of the bulk samples, heating/ cooling rate 20 deg/min: (a) heating; (b) cooling.

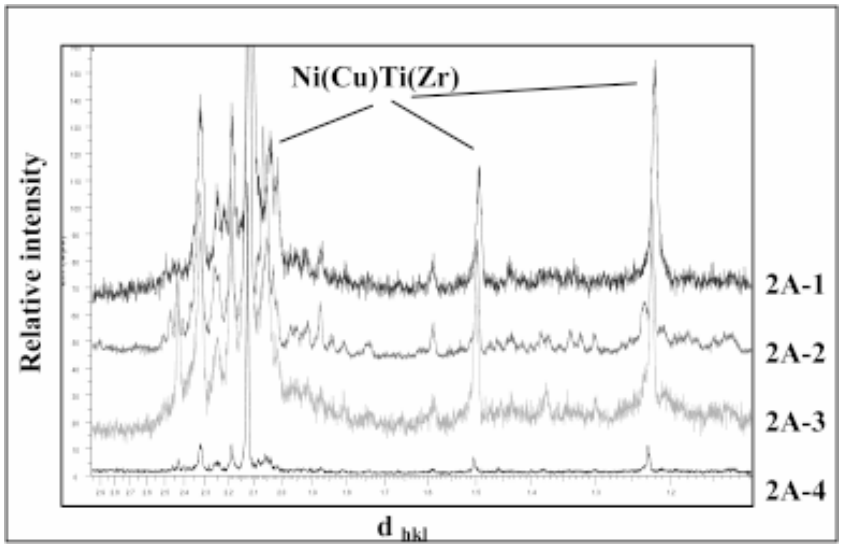


**Fig. 2.** X-ray diffraction from the massive samples; Ni(Cu)Ti(Zr) cubic phase is marked.

system and scanning Philips XL30 were used to study the microstructure. Calorimeters DSC Q1000 and SDT Q600 (TA Instruments) were applied for the thermal analysis. The Vickers microhardness and Young modulus were measured with Shimadzu DUH 202 ultra-micro hardness tester. The 20 G (200 mN) load was applied. The average *HV* and *E* values were obtained in 20 measurements on different parts of the cross-sections of the ribbons.

## 3. RESULTS

### 3.1. Composition, thermal analysis and phase composition of the bulk samples

The real chemical composition of the investigated alloys, determined with EDS method was $(Ni_{1-x}Cu_x)_{60.0}Zr_{17.8\pm0.5}Ti_{13.4\pm0.05}A1_{4.8\pm0.3}Si_{4.1\pm0.2}$ with $x$ = 0.13, 0.28, 0.45, and 0.64, for alloys marked as 2A-1, 2A-2, 2A-3 and 2A-4 respectively.

The thermal curves resulting from the melting and crystallization of the rapidly solidified massive samples, measured at the rate of heating and cooling 20 deg/min are presented in Figs.1a and 1b. Except for the main peak concerning melting of an eutectic, two thermal effects are present in the higher temperatures, related to the melting of the solid solutions, revealing heat effects increasing with the Cu content increase (Fig. 1a). It is also visible that during cooling, the double thermal effect concerning eutectic crystallization from the melt changes in the alloys 2A-1 and 2A-2 to the single one in the samples 2A-3 and 2A-4, suggesting transition from two slightly different unequilibrium eutectic compositions to a single one, together with the increasing amount of the crystallization of the two other phases (Fig. 1b). Together with the Cu content increase, both solidus ($T_s$) and liquidus ($T_l$) temperatures gradually decrease from 1000 to 973 °C and from 1183 to 1152 °C respectively, (Table.1).

X-ray phase analysis from the massive samples (Fig. 2) showed the same phase sequence for all samples 2A-1 to 2A-4 that have been solidified at similar cooling rates in the copper mould. A main difference concerns the amount of the amorphous phase retained, the lowest for the 2A-4 sample containing 23 at.% of Cu. The cubic NiTi(Cu,Zr) crystalline phase only could be identified in the samples. The other phases could not be identified as equilibrium ones.

The SEM microstructure of the bulk samples revealed variations of the contrast achieved from the amorphous matrix and differences in the local density of the crystallization centers, suggesting element segregation in the liquid phase (Fig. 3a). The crystallites revealed dendritic shape (Fig. 3b). Both the different contrast and the EDX compositions measurements suggest that two types of the dendrites predominantly crystallized from the melt. The $(Ni_4Cu)_{53}(Zr_2TiAl)_{40}Si_7$ and $(Ni,Cu)_{40}Zr(Ti)_{35}Si_{25}$ compositions were determined.

**Table 2.** Parameters connected to the GFA of the alloys: supercooled liquid range $\Delta T = (T_x - T_g)$, reduced glass transition temperature $T_g/T_l$, reduced crystallization temperature $T_x/(T_g+T_l)$, *HV* and Young modulus.

| Alloy | $\Delta T$ [deg] | $T_g/T_m$ | $T_x/(T_g+T_l)$ | *HV* [GPa] load of 20 G | *E* [GPa] load of 20 G |
|---|---|---|---|---|---|
| **2A-1** | 12.7 | 0.65 | 0.37 | 8.04 | 116.96 |
| **2A-2** | 11.6 | 0.65 | 0.37 | 7.86 | 101.89 |
| **2A-3** | 22.9 | 0.64 | 0.37 | 7.91 | 102.65 |
| **2A-4** | 19.9 | 0.65 | 0.37 | 7.76 | 97.67 |

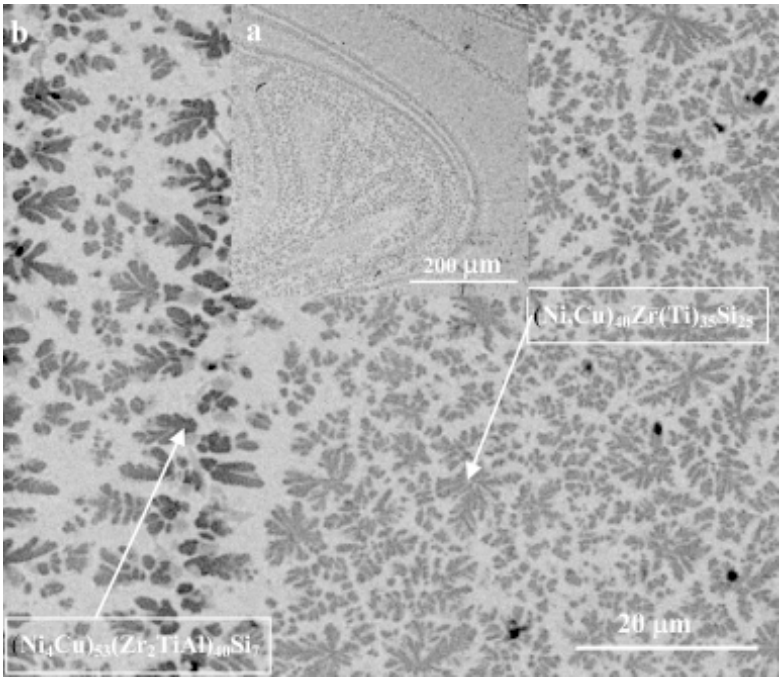


**Fig. 3.** SEM microstructure of the bulk sample of the alloy 2A-1 (a) general view and (b) dendritic microstructure.

## 3.2. The structure and thermal analysis of the ribbons

The structure of the ribbons was controlled by X-ray diffraction and TEM. In the case of all investigated alloys X-ray diffractions (Fig. 4a) electron diffraction patterns and homogenous contrast in TEM bright and dark field images (Figs. 4b and 4c), were typical for the amorphous structures. As no crystalline phase was detected with TEM, the small peaks superimposed to the amorphous broad peak observed for the 2A-1 sample could be attributed to the surface oxides.

DSC curves concerning glass transition and crystallization of the ribbons during heating are presented in Fig. 5, and the results in Tables 1 and 2. The curves show that the increase of the Cu content to 13 at.% leads to the crystallization process proceeding in three thermal effects, similarly to the crystallization from the melt (Fig. 1b) and in a wider temperature range, in comparison with 2A-1 alloy containing 8 at.% of Cu. Together with the increase

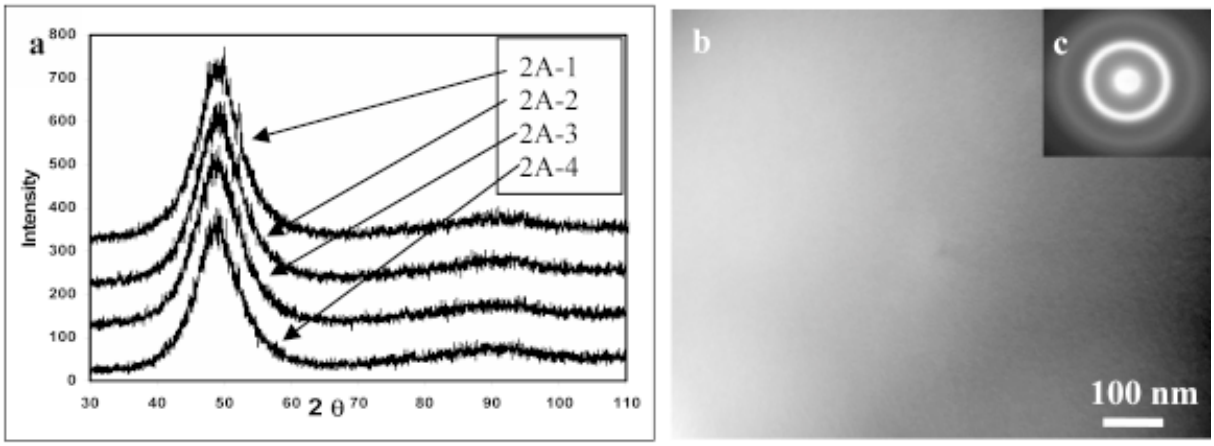


**Fig. 4.** (a) X-ray diffraction from the ribbons 2A-1 -2A-4; (b) TEM bright field, and (c) electron diffraction from the ribbon 2A-2.

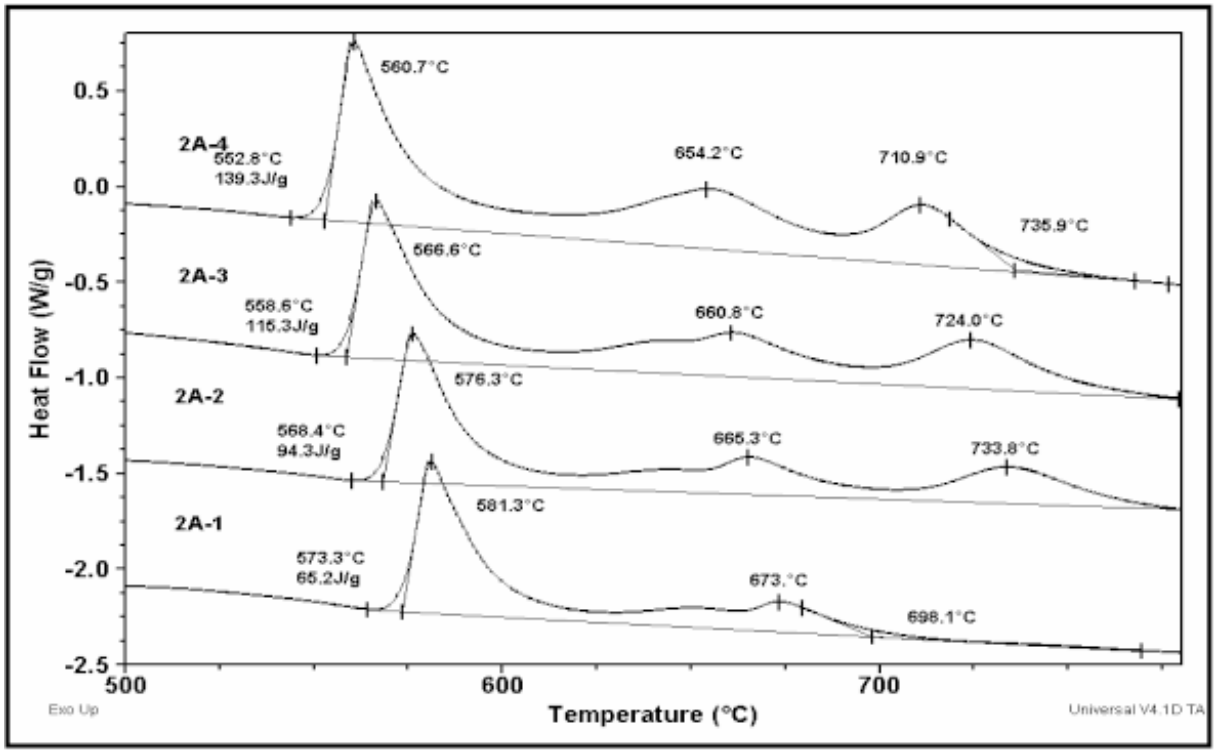


**Fig. 5.** DSC curves presenting glass transition and crystallization of the ribbons (heating rate 20 deg/min).

of Cu content in the ribbons the primary crystallization temperature $T_x$ (measured as the onset temperature) decreases systematically while total enthalpy of crystallization increases. On the other hand the separate enthalpy of primary crystallization reveals only small increase. Glass transition temperature $T_g$ reveals the same tendency as crystallization and melting temperatures of the alloys, and decreases systematically together with Cu content increase (Table 1). As a result quantities related to the glass forming ability (GFA) $T_g/T_m$ and $T_x/(T_g+T_l)$ [10] remain constant, on the level 0.65 and 0.37 respectively. The overcooled liquid range $\Delta T$ increases together with Cu content (Table 2).

### 3.3. Microhardness of the ribbons

The microhardness and elastic modulus of the ribbons are presented in Table 2. The microhardness decreases only slightly, in the range of 8.0 – 7.8

GPa. The Young modulus decrease is more evident, as well as with the Cu content increase.

## 4. DISCUSSION OF THE RESULTS

It is generally accepted that the large differences in the constituent atom sizes play an important role in the increasing glass forming ability of the alloys [11]. Ni and Cu atoms however, reveal similar diameter and complete solubility in the binary phase diagram. This explains the constant values of the parameters connected to glass forming ability (except D*T*) independently from the Cu content (Table 2). Nevertheless, increasing Cu addition influences thermal stability of the phases, decreasing temperatures of solidus, liquidus end the eutectic temperature. The observed splitting of the thermal effect connected to the eutectic crystallization from the melt in alloys 2A-1 and 2A-2 agrees well with the segregation in the liquid phase observed in the bulk samples of the same alloys, solidified with the high cooling rates (Figs. 1b and 3a). As far the authors know, such segregation was not observed in the basic NiTiZrSi amorphous compositions and may be most probably attributed to the Al content. The increasing Cu content suppresses this tendency. There was no difference in the amorphous structure of the ribbons, but in the irregular increase of the supercooled range $\Delta T$ and decrease of the glass transition and primary crystallization temperatures. The crystallization of the glass seems to involve more complicated processes, also including an increase in enthalpy together with the Cu increase. What concerns the bulk samples is that their structure remains partially amorphous. It is visible from Fig. 2 that the amount of the amorphous phase remained similar in alloys 2A-1 to 2A-3 but decreased drastically in alloy 2A-4 containing 25 at.% Cu. This observation has no explanation in the parameters connected to the GFA of the alloys, however it may be explained assuming that Cu atoms supply the crystallization centers as well in Ni-based as in Fe-based amorphous alloys [12]. The composition of the main crystalline phases (dendrites) identified in the bulk samples was $(Ni_4Cu)_{53}(Zr_2TiAl)_{40}Si_7$ (cubic solid solution) and $(Ni,Cu)_{40}Zr(Ti)_{35}Si_{25}$.

It seems from the microhardness test that increase of Cu addition only slightly lowers the mechanical properties of the amorphous phases. As far as it concerns mechanical properties and the crystalline phases of partially amorphous bulk samples, further investigations are necessary.

## ACKNOWLEDGEMENTS

This work was supported by the Polish Ministry of the Science and the Information Society Technologies as the Research Project No.3 T08A 067 28.

Financial support from the European Union (Project MCRTN-CT-2003-504692) is gratefully acknowledged.

## REFERENCES

[1] S. Pang, T. Zhang, K. Asami and A. Inoue // *Materials Science and Engineering A* **375-377** (2004) 368.

[2] J. K. Lee, D. H. Bae, W. T. Kim and D. H. Kim // *Materiale Science Engineering A* **375-377** (2004) 332.

[3] T. G. Park, S. Yi and D. H. Kim // *Scripta Mater.* **43** (2000) 109.

[4] D. V. Louzguine-Luzgin, T. Shimada and A. Inoue // *Intermetallics* **13** (2005) 1166.

[5] Tao Zhang and Akihisha Inoue // *Materials Trans.* **43** (2002) 708.

[6] Shujie Pang, Tao Zhang, Katsuhuko Asami and Akihisa Inoue // *Materials Trans.* **43** (2002) 1771.

[7] Chaoli Ma, Hideoki Soejima, Satoru Isihara, Kenji Amiya, Nabuyaki Nishiyama and Akihisa Inoue // *Materials Transactions* **45** (2004) 3223.

[8] M.H. Lee, W. T. Kim, D. H. Kim and Y. B. Kim // *Materiale Science Engineering A* **375-377** (2004) 336.

[9] H. Choi-Yim, R.D. Conner and W.L. Johnson // *Scripta Materialia* **53** (2005) 1467.

[10] P. Lu and C.T. Liu // *Acta Materialia* **50** (2002) 3501.

[11] A. Inoue // *Mater. Trans., JIM* **36** (1995) 866.

[12] M. E. McHenry, F. Johnson, H. Okamura, T. Ohkibo, V. R. V. Ramanan and D. E. Laughlin // *Sripta Materialia* **48** (2003) 881.